Discovery of an Orally Available STING Agonist BSP16 as a Preclinical Immunotherapy Drug Candidate

Ying Meng[2], Tiejun Bing[2], Dongyu Liu[1], Zhiyu Li[1], Jinlei Bian[1*]
[1]Department of Medicinal Chemistry, School of Pharmacy, China Pharmaceutical University, Nanjing, China
[2]International Department, ICE Bioscience Inc., Beijing, China

ICE Bioscience — Innovative CRO+Explorer

中国药科大学 CHINA PHARMACEUTICAL UNIVERSITY

Abstract

STING agonism has emerged as a promising therapeutic approach for cancer treatment via activation of the host antitumor immune response. Herein, we present a potent STING agonist BSP16 developed based on our STING agonist screening platform. It was demonstrated that BSP16 could effectively bind to STING protein and induce the active conformational transition of STING. In IRF reporter assay, BSP16 strongly activated STING signaling in both human and mouse cells with EC50 = 9.2 μM and 5.7 μM, respectively. The capability of BSP16 to activate STING pathway *in vitro* was also validated by its regulation of downstream gene transcription and protein expression. In addition, BSP16 had a favorable druggability, including good water solubility, good membrane permeability, good stability, no hERG toxicity, and no CYP3A4 inhibitory activity. In terms of the PK profiles, the exposure of BSP16 *in vivo* was excellent when administered intravenously and orally and the oral bioavailability of BSP16 was extremely high (F = 107%). Most importantly, BSP16 was proven to be effective in multiple syngeneic models, and in some cases, BSP16 could induce complete tumor regression and durable antitumor immune memory. Moreover, the synergistic antitumor effect of BSP16 combined with anti-PD-L1 therapy in the humanized mouse model of HCC827 lung cancer proved the potential benefits of BSP16 in combination with immune checkpoint inhibitors.

In summary, BSP16 is a promising STING agonist with outstanding *in vitro* and *in vivo* activities and favourable druggability, which makes it valuable for further development as a novel anticancer agent.

Background

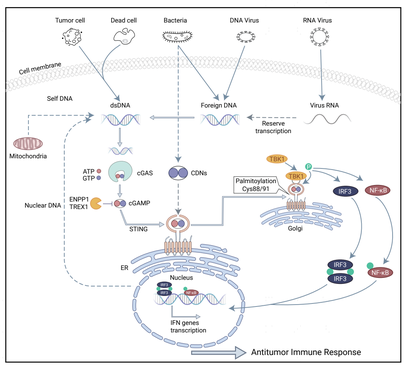

The cGAS-STING pathway is initiated in response to aberrant cytosolic DNA signals, followed by the generation of cGAMP as a second messenger. cGAMP then binds to and activates STING protein, which further triggers the activation of downstream TBK1, IRF3 and NF-κB. The activated transcription factors subsequently enter the nucleus and induce the expression of type I interferon responsible for the antitumor immune reaction.

BSP16 efficiently activates the STING signalling pathway

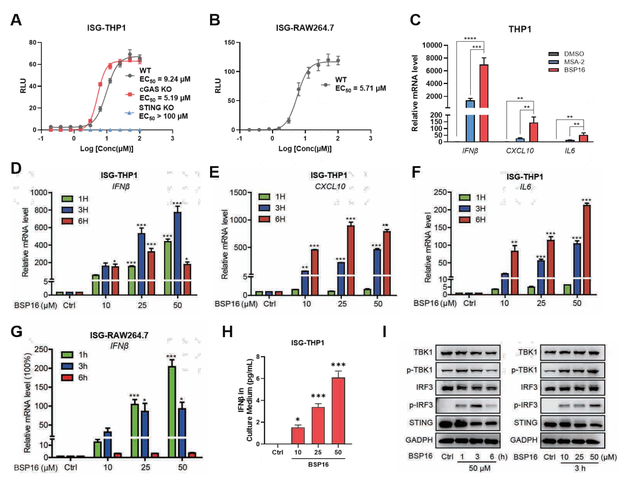

Figure 1. Cell-based activities of BSP16. Luciferase reporter activities of BSP16 in (A) human-derived ISG-THP1 cells and (B) murine-derived ISG-RAW264.7 cells. (C) qRT-PCR analysis of target gene expression in THP1 cells treated with BSP16 or MSA-2 in 3 h. (D-F) qRT-PCR analysis of the time-dependent and dose-dependent target gene expression in ISG-THP1 cells treated with BSP16. (G) qRT-PCR analysis of IFN β gene expression in ISG-RAW264.7 cells treated with BSP16 . (H) BSP16 induced IFNβ secretion in ISG-THP1 cells in a dose-dependent manner. (I) Western blot analysis of the time-dependent and dose-dependent protein expression in STING-TBK1-IRF3 axis in ISG-THP1 cells stimulated with BSP16.

BSP16 shows a favorable druggability

Table 1. Selected ADMET properties of BSP16.

Compd.	Aq. Solubility		LogP	PAMPA (10^{-6} cm/s)	PP FF(%)	RLM CL_{int} (L/h/kg)	hPlasma(%)	THP1 CC_{50}(μM)	CYP3A4 Inhibition (%@10uM)	hERG (%@10uM)
	Water (mg/mL)	PBS (mg/mL)								
BSP16	0.70	1.6	2.4	2.04	0.07	0	0	>100	13.47	-0.70

BSP16 exhibits good pharmacokinetic profiles

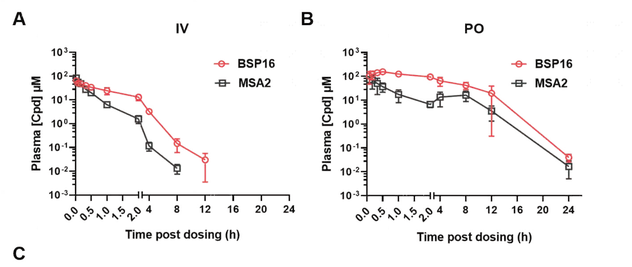

C

Compd.	Route	C_{max} (mg L^{-1})	T_{max} (h)	AUC_{0-t} (h μg mL^{-1})	$AUC_{0-\infty}$ (h μg mL^{-1})	$t_{1/2}$ (h)	V (L kg^{-1})	CL (L h^{-1} kg^{-1})	$MRT_{0-\infty}$ (h)	F (%)
BSP16	iv (5 mg/kg)	/	/	29.43	29.45	1.04	0.26	0.17	1.39	/
	po (50 mg/kg)	58.2	0.42	315.92	315.95	1.60	0.38	0.16	5.05	107

Figure 2. Pharmacokinetic data of BSP16 in SD rats (n = 3). (A-B) Obtained concentration-time curve after a single intravenous (5 mg/kg) or oral (50 mg/kg) administration of BSP16 or MSA-2. BSP16 shows a comprehensively improved exposure (AUC) compared with MSA-2. (C) Selected pharmacokinetic parameters of BSP16.

BSP16 exhibits a promising antitumor activity in the MC38 syngeneic model

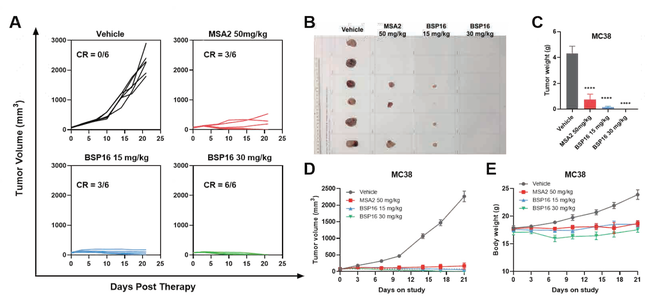

Figure 3. *In vivo* antitumor activity of BSP16 in the MC38 syngeneic mice model with the treatment of BSP16 or MSA-2 (Q3D PO) (n = 6). (A) Individual tumor growth of MC38 tumor. (B-C) All mice were euthanized and tumors were taken out on day 21. Tumors were photographed and weighed. (D) Average tumor size change during the therapy. (E) Bodyweight change of MC38 bearing mice during the therapy.

BSP16 shows a significant inhibitory effect on CT26 tumor in vivo and in situ

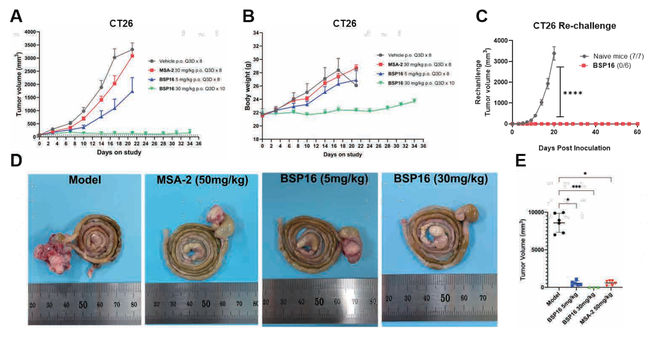

Figure 4. BSP16 inhibits the growth of CT26 tumor in vivo (A-C) and in situ (D-E). (A) Average tumor size change. (B) Bodyweight change of CT26 bearing mice. (C) Mice with complete tumor regression were rechallenged with CT26 after 21 days and compared with the naïve mice. (D) Representative images of CT26 orthotopic tumors with different treatments on day 25. (E) Volume of CT26 orthotopic tumors on day 25.

BSP16 kills tumors by activating antitumor immunity

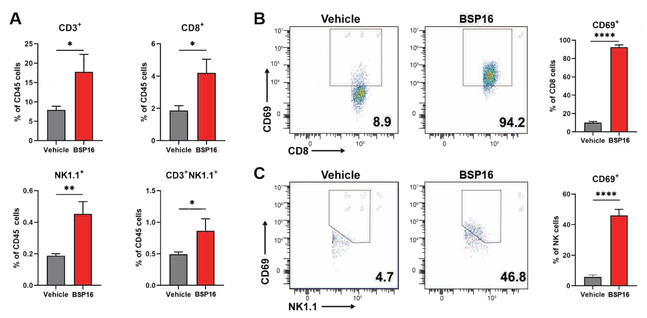

Figure 5. Lymphocyte immunophenotype of BSP16 in the MC38 syngeneic model. (A) Proportion of CD3+, CD8+, NK1.1+, CD3+NK1.1+ cells in total CD45+ lymphocytes in spleen of MC38 tumor-bearing mice. (B-C) Proportion of CD69+ cells in total CD8+ T and NK cells in spleen of tumor-bearing mice.

BSP16 inhibits progression of HCC827 lung cancer in a humanized mouse model

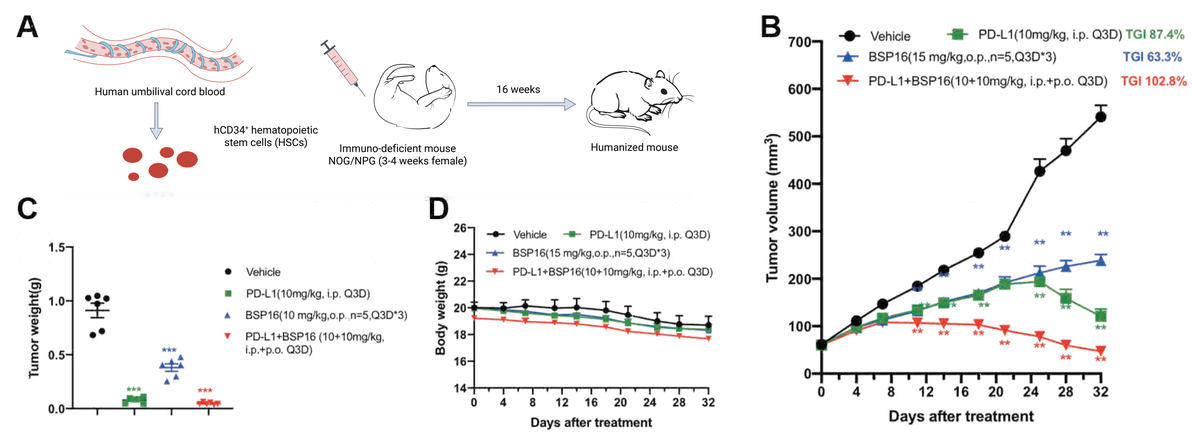

Figure 6. Activity of BSP16 combined with PD-L1 monoclonal antibody in HCC827 humanized mouse model. (A) Construction of a humanized mouse model. (B) Average tumor size change with indicated treatments. (C) Tumor weight of HCC827-bearing mice on day 25. (D) Body wight change of tumor-bearing mice during the therapy.

Conclusions

An orally available anticancer agent targeting STING adaptor is reported herein with:

- Good STING binding properties
- Excellent STING activation capabilities in vitro
- Favorable druggability and PK profiles
- Outstanding antitumor efficacy in vivo and in situ
- Promising potential of combination with immune check point inhibitors

References

1. Nature 2019, 574, 45
2. J Hematol Oncol 2019, 12, 35
3. Annu Rev Biochem 2022, 91, 599
4. Drug Discov Today 2020, 25, 230
5. Science 2020, 369, eaba6098
6. J Med Chem 2022, 65, 15048